

NMR STUDIES OF BENZENE ADSORBED ON SYNTHETIC FAUJASITE-TYPE ZEOLITES*

Shang-Bin LIU^a, Jin-Fu WU^{a,b}, Long-Ja MA^a, May-Whei LIN^a and Tun-Li CHEN^b

^a Institute of Atomic and Molecular Sciences, Academia Sinica,
P.O. Box 23-166, Taipei, Taiwan 10764, R.O.C.

^b Department of Chemistry, Tamkang University, Tamsui, Taiwan, R.O.C.

Received September 13, 1991

Accepted October 22, 1991

The sorption and transport properties of benzene on dehydrated NaX and NaY zeolites have been investigated directly by ¹H and ¹³C NMR measurements of the adsorbed benzene and probed indirectly by ¹²⁹Xe NMR of the coadsorbed xenon. Dehydrated NaX and NaY zeolite adsorbate samples containing various adsorbate concentrations and having various sample bed configurations, which were subjected to different preparatory and experimental conditions, have been examined. Thermal treatment at a temperature (>250°C) much greater than the boiling point of bulk benzene (80°C) for an extended period of several hours is indispensable to ensure a homogeneous benzene distribution within the supercages of the faujasite-type zeolites.

The study of sorption and transport phenomena of hydrocarbons through micro-porous zeolite particles is provoked not only by scientific interest but also by the demands of practical applications. Recently, the sample activation dependence of the distribution of organic adsorbates, namely hexane, 1,3,5-trimethylbenzene, hexamethylbenzene, and benzene within the supercage of powdered NaY zeolite have been examined by Pines and co-workers^{1,2} using ¹²⁹Xe NMR and ¹H multiple-quantum NMR spectroscopy, respectively. Specifically, the effect of sample pre-treatment on the distribution of benzene within the supercage of NaY zeolite (Si/Al = 2.49) was reexamined and confirmed by ¹²⁹Xe NMR and adsorption isotherms of coadsorbed xenon in conjunction with ¹H and ¹³C NMR of adsorbed benzene.³ These studies indicated that the assumption of a uniform molecular distribution upon adsorption on zeolite is questionable. A similar statement applies for the smaller, polar water molecules adsorbed on NaY zeolite.⁴ However, recent FTIR measurements⁵ on the adsorption of benzene on faujasite-type zeolites using thin platelets resulted in no change of IR spectra after either protracted exposure or intermittent heating of the samples. Therefore, additional evidence is required to resolve the discrepancies between the NMR and IR results.

* Presented as a poster at the International Symposium "Zeolite Chemistry and Catalysis", Prague, September 8-13, 1991.

We report here an extensive investigation of the adsorptive properties of benzene on NaX and NaY zeolites for which the samples contained various concentrations of adsorbate molecules subjected to various preparatory and experimental conditions; we examined these samples by ^{129}Xe , ^1H , and ^{13}C NMR spectroscopy.

EXPERIMENTAL

Powdered NaX (Si/Al = 1.23) and NaY (Si/Al = 2.49 and 2.70) zeolites (Strem Chemicals, Inc.), all having an average crystalline diameter ca 1 μm , were used as the adsorbents. Before adsorption of guest molecules, a known amount (typically ca 1 g) of hydrated zeolite sample in the sample tube was dehydrated by gradual heating to 400°C in vacuum ($<10^{-3}$ Pa) and was then maintained at this temperature for at least 15 h. Each sample was normally handled in a 10 mm NMR tube joined to a vacuum valve, the design of sample tube provided an easy setup for adsorption or desorption of adsorbate molecules and for isolation of the sample from the atmosphere during NMR experiments. The NMR sample tube had an overall length about 250 mm with sample packing height about 35 mm (deep bed sample configuration; DBC). In order to check the effect of sample bed height on benzene adsorption and related transport behavior, some samples were prepared in a 125 ml Erlenmeyer flask. The flat-bottom flask had an inner diameter about 55 mm and the resultant sample packing height was less than 2 mm (shallow bed sample configuration; SBC).

After dehydration, benzene guest molecules (adsorbate) were introduced into the samples of host NaX and NaY zeolites (adsorbents) by vapor transport at room temperature (22°C). The exact amount of benzene coverage was determined gravimetrically; the average number of benzene molecules in each zeolite supercage is hereafter denoted θ . For samples prepared by SBC, the benzene/zeolite sample was transferred into NMR sample tubes under atmosphere of dry nitrogen in a glove box immediately after adsorption of benzene. The nitrogen gas was then evacuated before adsorption of xenon or any further sample treatment. Further coadsorption of gaseous xenon onto the benzene/zeolite sample was done in the vacuum apparatus; the equilibrium pressure of xenon was measured on an absolute-pressure transducer. Further thermal treatment of the adsorbate/adsorbent samples was done in a furnace regulated by a programmable temperature controller.

All NMR experiments were done on a spectrometer (Bruker MSL-300) using a broadband NMR probe with the proton-decoupling option. The field strength of the wide-bore superconducting magnet is 7.05 Tesla, corresponding to resonance frequencies 300.13, 75.47, and 83.01 MHz for the nuclei ^1H , ^{13}C , and ^{129}Xe respectively. For the ^{129}Xe NMR experiments, free induction decays (FID) were recorded at 22°C following a single radio-frequency pulse (ca 30°) at 0.3 s intervals. We followed this procedure because the adsorbed xenon has a large spin-lattice relaxation time ($T_1 \geq 3$ s). Typically, 1 000–240,000 FID were accumulated depending on the amount of xenon adsorbed on the sample and on the resultant linewidth of the NMR spectrum which affected the signal-to-noise (S/N) ratio of the resonance signal. The chemical shifts of ^{129}Xe were referred to that of gaseous xenon at zero density according to the equation given by Jamesen.⁶ All resonance signals of ^{129}Xe adsorbed on the samples were shifted to higher frequency relative to the reference, which we define to be the positive direction. The ^1H NMR spectra were also obtained by the single-pulse sequence using a 2 s recycle delay. A number of 120 accumulated FID were typically adequate to generate spectra with adequate S/N ratio. The ^{13}C NMR spectra, on the other hand, were obtained with proton decoupling; 12,000 scans were typically averaged every 0.6 s. The reference for the chemical shifts

of both ^1H and ^{13}C was liquid benzene (adjusted to tetramethylsilane, or TMS, as standard) at the same spectrometer settings.

RESULTS AND DISCUSSION

Figure 1 displays the room temperature ^{129}Xe NMR spectra of xenon (equilibrium pressure 300 Torr, 1 Torr = 0.133 kPa) in dehydrated NaY zeolite [Si/Al = 2.49, denoted NaY (2.49)] with and without benzene adsorption, recorded immediately after sample preparation and without thermal treatment. All spectra shown in Fig. 1 and in subsequent figures are plotted such that all NMR spectra in the same figure are normalized to the greatest peak in each spectrum. Fig. 1a is the ^{129}Xe spectrum obtained before benzene adsorption (i.e. $\theta = 0$). The xenon atoms (kinetic diameter $d_0 = 0.396$ nm), like benzene molecules ($d_0 = 0.585$ nm), can be adsorbed only into the supercages of faujasite-type zeolites (channel aperture ca 0.74 nm), as for reasons of size they cannot enter the sodalite cage or the hexagonal prism which have an entrance aperture only ca 0.26 nm.⁷ Hence the observed ^{129}Xe resonance in Fig. 1a, linewidth $\Delta\omega \approx 2$ ppm (measured at full-width half-maximum; FWHM) and chemical shift $\delta = 74$ ppm, therefore arises from the collision of xenon atoms with the zeolite walls and xenon-xenon interactions within the NaY(2.49) supercage. The sharp resonance line in Fig. 1a indicates that, although xenon experiences many

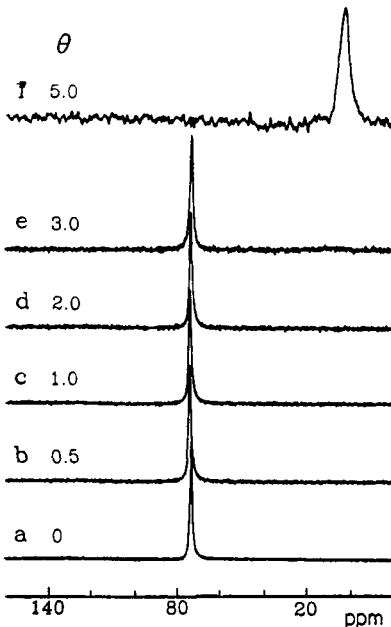


FIG. 1

Room temperature (22°C) ^{129}Xe NMR spectra of xenon (equilibrium pressure 300 Torr) coadsorbed on dehydrated benzene/NaY(2.49) in absence of sample treatment under DBC. Spectra recorded a without loading benzene, b-f immediately after loading benzene. All spectra (and the subsequent NMR spectra in the other figures) are normalized so that the major resonance peak has a uniform height

collisions at locally different sites, ^{129}Xe resonance is capable of detecting an average environment, on the time scale of NMR experiments, weighted by the collision probability at each site.

Spectra in Fig. 1b–1e were recorded immediately after introduction of benzene to the DBC NaY(2.49) zeolite without any sample pretreatment. That the observed linewidths and chemical shifts are nearly identical to that of Fig. 1a indicates that, within the detectable sample range which is confined by the length of the NMR coil (ca 25 mm), the contribution to the ^{129}Xe resonance from xenon coexisting with benzene within NaY(2.49) supercage can be excluded. That is, the benzene molecules are probably adsorbed on the external surface (or intercrystalline voids) of the zeolite crystallites. Moreover, as is discussed later, the existence of a gradient of adsorbate concentration along the sample bed is not precluded to explain this observation. At the greatest coverage of benzene, the broad line in Fig. 1f, $\delta \approx 10$ ppm (near that of gaseous xenon reference at 0 ppm), arises from xenon adsorbed in the voids between zeolite crystallites.^{8,9} In other words, the entrances to the zeolite supercage were blocked by benzene molecules adsorbed either within or outside of the zeolite crystallites and hence prevented xenon atoms from entering the supercage. Because mobile gaseous (free) xenon atoms can move rapidly into and out of the sample (and hence the surrounding NMR coil) and has $T_1 > 30$ s, much greater than our sampling cycle 0.3 s, it is unlikely to be observable. We show later that, even if the gaseous xenon peak appears, the line is much narrower and is expected to be located near 0 ppm.

The effect of thermal treatment (heating temperature hereafter denoted by T_s) on the room-temperature ^{129}Xe spectra of xenon (300 Torr) coadsorbed in the DBC benzene/NaY (2.49) system is exemplified in Fig. 2 for two different benzene loadings ($\theta = 1.0, 2.0$). The bottom spectra in Fig. 2a and 2b were both recorded immediately after the introduction of benzene to the sample without further thermal treatment (i.e. $T_s = 22^\circ\text{C}$). The spectra of the corresponding samples recorded after consecutive thermal treatments are also shown in Fig. 2. Upon increasing $T_s < 200^\circ\text{C}$, that benzene molecules migrate into the NaY supercages is evident by the broadening of the NMR lines. The fact that the ^{129}Xe NMR spectrum shows no further change for $T_s \geq 200^\circ\text{C}$ (Fig. 2) therefore indicates a trend toward a homogeneous distribution of benzene molecules within the zeolite supercages; no further change in the ^{129}Xe spectrum is visible for $T_s \geq 300^\circ\text{C}$. Such variation of benzene adsorption states were also sometimes followed by the xenon adsorption isotherm measurements which have been shown previously;³ we found that, upon increasing $T_s < 150^\circ\text{C}$, the respective sample showed an increase in xenon adsorption and for $T_s \geq 200^\circ\text{C}$ the adsorption curves showed no further change (cf. Fig. 2 in ref.³). Similar conclusions can also be drawn for samples with other coverages of benzene and for benzene adsorbed on DBC NaX (1.23) and DBC NaY (2.70) zeolites, as depicted in Fig. 3. The onset $T_s \approx 250^\circ\text{C}$ to obtain a homogeneous sample distribu-

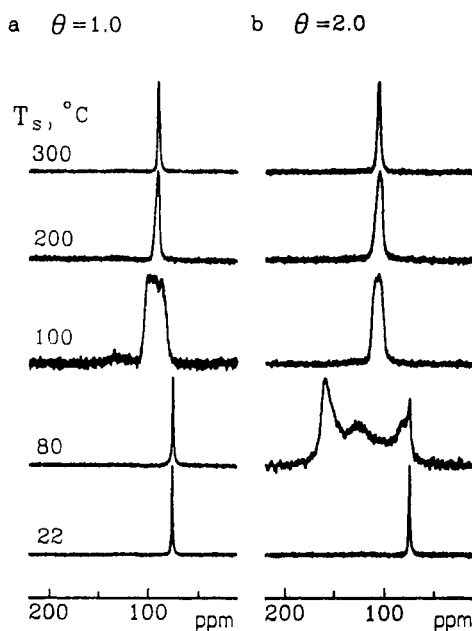


FIG. 2

The effect of sample treatment, by heating at temperature T_s for 1 h, on the ^{129}Xe NMR spectra of xenon (300 Torr) coadsorbed in DBC benzene/NaY(2.49) samples with average benzene coverage a $\theta = 1.0$, b $\theta = 2.0$; spectra at bottom ($T_s = 22^\circ\text{C}$) were obtained after dosing benzene without thermal treatment

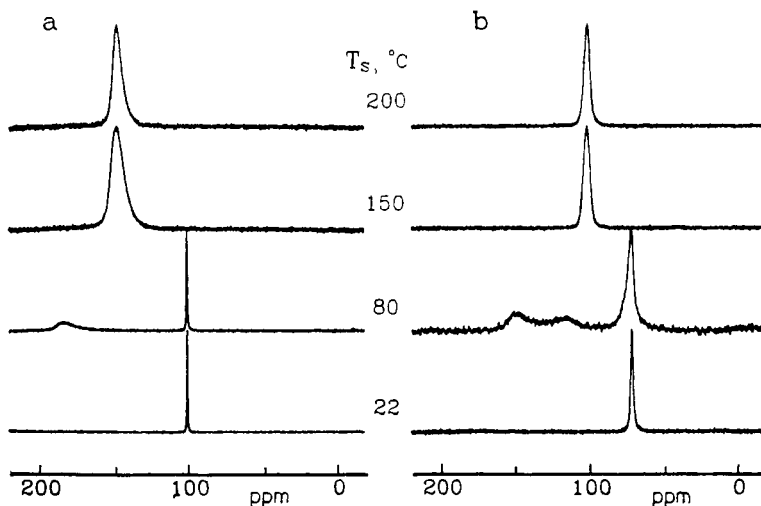


FIG. 3

Similar to Fig. 2, but for a DBC benzene/NaX (1.23) and b DBC benzene/NaY (2.70) systems; both with average benzene coverage $\theta = 2.0$

tion observed in this study is supported by the previous UV and IR measurements made by Primet et al.¹⁰ Based on their UV and IR spectra obtained from the progressive adsorption and desorption of benzene in NaX (Si/Al = 1.23) and NaY (Si/Al = 2.43), these authors concluded that at room temperature benzene molecules adsorbed irreversibly on the Na^+ cations sites within the zeolite supercage. The authors further found that, upon desorption by sample evacuation at elevated temperatures, complete removal of benzene requires a temperature of 150°C for NaX and 250–300°C for NaY.

Comparing the spectra in Fig. 2a and 2b for $T_s \geq 200^\circ\text{C}$, we see that the observed chemical shift $\delta(\theta = 2.0) > \delta(\theta = 1.0)$ at the same xenon loading pressure is due mainly to the varied concentration of adsorbate present in the samples. Moreover, for samples with different adsorbent but with the same adsorbate concentration (θ) at the same xenon loading pressure, e.g. for $\theta = 2.0$ in Fig. 2b and Figs 3a and 3b, the observed ^{129}Xe chemical shifts follow $\text{NaX}(1.23) > \text{NaY}(2.40) \geq \text{NaY}(2.70)$ due to the difference in the number Na^+ cations present in each zeolite samples. This result is contrary to the previous observations by Ito and Fraissard¹¹ who concluded that, at constant xenon density, the ^{129}Xe NMR chemical shift is independent of the Si/Al ratio of faujasite-type zeolites.

The significance of the thermal treatment on the equilibrium distribution of benzene inside zeolite supercages is further supported by a “long-term” experiment shown in Fig. 4 for DBC benzene/NaY(2.49) samples; similar results were found for the sample systems DBC benzene/NaX(1.23) and DBC benzene/NaY(2.70). In the “long-term” experiments, samples were kept undisturbed at 22°C after the adsorption of benzene followed by adsorption of xenon at an equilibrium pressure of 300 Torr. The ^{129}Xe NMR spectrum was recorded after varied sample resting periods (denoted t_d , in days) ranging from as brief as a few hours (i.e. $t_d = 1$) to as long as 120 days. For comparison, the top spectra in Fig. 4a and 4b were recorded after both samples were heated at 250°C for 10 h; the measured values of their line-widths and chemical shifts are nearly identical to the corresponding sample observed in Fig. 2 for $T_s = 300^\circ\text{C}$, as expected. The spectra in Fig. 4 clearly show that, without thermal treatment of the sample, benzene molecules migrated slowly into the DBC NaY(2.49) supercages and that an additional sample thermal treatment is required to ensure a homogeneous adsorbate distribution. Similar phenomena occur in samples with varied benzene loadings.

The broad peak with the greatest chemical shift in Fig. 4b commonly appeared in the spectra of other samples with varied θ , especially for samples having insufficient thermal treatment or resting after an extended period t_d . As a matter of fact, according to the ^{129}Xe NMR results gathered from all the DBC benzene/NaY(2.49) samples examined in this study, a threshold occurred for samples initially loaded with $\theta \geq 2.5$ up to saturation coverage of benzene and in the absence of thermal treatment, a weak broad peak appeared at $\delta \approx 160–200$ ppm on most occasions

when coadsorbed with 300 Torr xenon. The above value of δ , which normally depended on experimental conditions (see later discussion), corresponded to samples (coadsorbed with 300 Torr xenon) having a "homogeneous" distribution of benzene (e.g. for samples thermally activated at 250°C for 10 h) within NaY(2·49) supercages with $\theta \geq 3\cdot8$ (ref.⁹). Possible origins for the appearance for such a peak at common locations demand closer examination. The chemical shift for bulk liquid xenon which normally occurred at a temperature much less (50–100°C) than the present experimental temperature (22°C) is ca 250 ppm (refs^{12–14}) and hence is unlikely to be responsible for the occurrence of the resonance peak. One might at first glance attribute this peak to xenon dissolved in bulk liquid benzene (ca 195 ppm).^{15,16} However, we cannot thereby explain that this resonance peak occurred at 195 ppm $< \delta < 220$ ppm which commonly appeared for DBC benzene/NaY(2·49) with $\theta \geq 3\cdot0$ prior to sample treatment. Furthermore, as the saturation coverage for benzene/NaY(2·49) is ca 4·9–5·2 molecules of benzene per supercage,^{9,17,18} this resonance peak might be due to xenon coadsorbed with benzene/NaY(2·49) with θ near saturation coverage. However, ¹²⁹Xe NMR of separate homogeneous benzene/NaY(2·49) samples⁹ exhibited two peaks at 204 and 10 ppm for $\theta = 4\cdot7$, but for $\theta > 5\cdot0$, only one peak located at $\delta \approx 10$ ppm was observed due to the lack of available space for xenon to adsorb within the NaY(2·49) supercage. Hence the

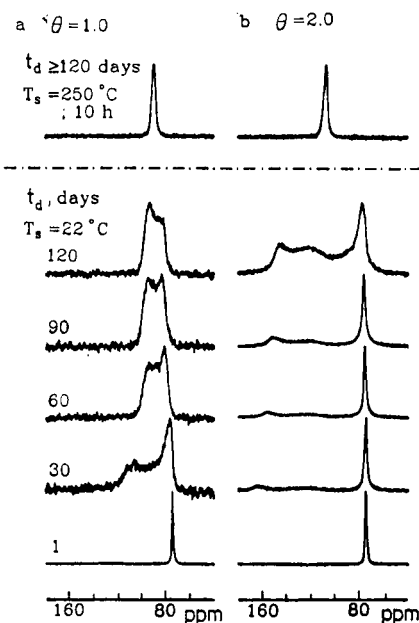


FIG. 4
Variation of ¹²⁹Xe NMR spectra (300 Torr xenon) of DBC benzene/NaY(2·49) sample a $\theta = 1\cdot0$, b $\theta = 2\cdot0$, after various resting periods t_d (in days) at room temperature ($T_s = 22^\circ\text{C}$). Bottom spectra were recorded immediately after dosing benzene ($t_d = 1$). Top spectra were recorded after $t_d \geq 120$ days and thermal treatment at $T_s = 250^\circ\text{C}$ for 10 h

proper assignment of the resonance peak to xenon coadsorbed with benzene within NaY(2·49) supercages is governed by the constraint that the range of benzene coverage was $4\cdot7 < \theta \leq 5\cdot0$. Alternatively, the benzene molecules perhaps acted as an adhesive by forming complexes with more than one Na^+ cation located at the external surface of different NaY(2·49) crystallites, hence forming zeolite aggregates of which the size of the intercrystalline voids slightly exceeding that of the supercages of the NaY(2·49); only in such an arrangement could xenon atoms be surrounded by benzene molecules with an average coverage $\theta > 4\cdot7$ hence the observed ^{129}Xe resonance line at $\delta > 204$ ppm. In support of this argument is that the zeolite powders of micrometer size commonly agglomerate to form sizable pellets (typically 2–3 mm, spherical in shape) at the top of the sample bed upon introduction of benzene; this behavior normally became more pronounced for samples dosed with large coverages of benzene. These arguments await further justification.

Despite some questions that remain to be answered, the above results nevertheless clarify the importance of thermal treatment on homogeneity of sample distribution. This effect, which has been largely overlooked, has been investigated for similar adsorbate/adsorbent systems^{1–4} using the same technique. However, this behavior was not reproduced by FTIR measurements on the same benzene/faujasite-type zeolites system using a relatively small amount (ca 10 mg) of sample in the shape of thin platelets⁵. In order to accentuate further the effects of sample bed configuration on the sorption and transport properties of benzene in faujasite-type zeolites, we performed separate NMR experiments to resolve this conflict. Before we proceed to describe the results of these experiments, we discuss probable schemes for the sorption and transport of benzene on microporous faujasite-type zeolites.

Sorption diffusivities, which characterize transport processes, were typically measured by uptake and NMR pulse-field-gradient measurements. For benzene adsorbed on faujasite-type zeolites, a large discrepancy has been found for intracrystalline diffusivities derived from the two techniques.¹⁹ Possible origins of this discrepancy arise from the existence of heat-transfer,^{20–21} mass-transfer,²² and surface barrier^{23–25} effects of the benzene/zeolite system. We envisage several extreme cases of adsorbate inhomogeneity (or state of non-equilibrium):

case I: the inhomogeneity is caused by the gradient of concentration of the adsorbates along the sample bed, as shown in Fig. 5a;

case II: the overall adsorbate concentration is “uniform” throughout the sample bed but the guest molecules are adsorbed on the external surfaces or intercrystalline voids of the zeolite crystallite, as in Fig. 5b, which may or may not block the channel apertures of the crystallite and hence the entrance of the xenon atoms;

case III: similar to case II, but the guest molecules are adsorbed in supercages which are located at the outer shell of the zeolite crystallite, as in Fig. 5c.

case IV: similar to case II, but the adsorbate distribution is inhomogeneous among supercages or intracrystalline voids of individual zeolite crystallites, as in Fig. 5d. In our experiments, all ^{129}Xe NMR spectra for the thermally well treated samples revealed a single peak which is characteristic of a uniform distribution of the adsorbate molecules over the entire zeolite cavities, as shown in Fig. 5e, whilst for samples having insufficient thermal treatment, hence not in a state of equilibrium, and described in the above cases of adsorbate inhomogeneities (or combinations of these cases), either a broaden resonance peak or multiple ^{129}Xe lines are observed.

In order to resolve the above cases of adsorbate inhomogeneity, we performed ^{129}Xe NMR of xenon coadsorbed on benzene/zeolite samples prepared in varied sample bed configuration and under various experimental conditions. In addition, ^1H and ^{13}C NMR spectra of adsorbed benzene on the corresponding zeolite adsorbents (without xenon) were also recorded, to which the ^{129}Xe results are correlated. Fig. 6 displays the ^{129}Xe NMR spectra (300 Torr xenon) of DBC benzene/NaY(2.49) sample with $\theta = 3.8$ under various sample preparation procedures, the spectra were also recorded at various sample tube positions relative to the NMR coil in order to render the axial adsorbate distribution of the sample bed; the respective sample positions applied are shown schematically on the left of the figure. As we described earlier, a typical sample filling height by DBC was ca 35 mm and

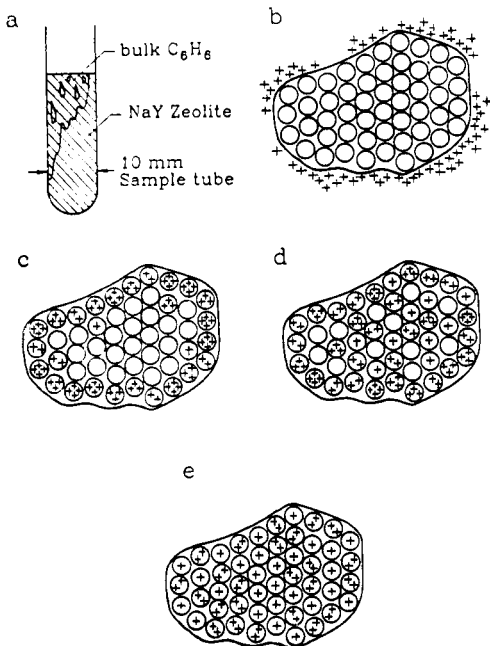


FIG. 5

Schematic drawings of the possible dispersion of benzene molecules on zeolites (see text). The adsorbate molecules may be distributed such that a macroscopic (bulk) concentration gradient exists along the sample bed, or have a 'uniform' overall concentration throughout the sample bed but b adsorbed on the external surfaces or intercrystalline voids, or c adsorbed in cages located at the outer shell, or d adsorbed inhomogeneously among cages or intracrystalline voids, or e distributed homogeneously in supercages of the zeolite crystallite. In drawings b–e, a specific average benzene (shown by the symbol +) loading $\theta \approx 1.5$ within supercage (open circles) of each zeolite crystallite is depicted

the length of the NMR coil is ca 25 mm. Spectra in Fig. 6a were obtained immediately after adsorption of benzene without further treatment. The middle spectrum in Fig. 6a represents a "normal" sample position; three resonance peaks at $\delta = 220$, 74 and 10 ppm are observed. The peaks at 74 and 10 ppm are attributed to resonance arising from xenon adsorbed in NaY supercages in the absence of benzene and to xenon adsorbed within the intercrystalline voids, respectively.^{8,9} The peak at 220 ppm, which has been discussed earlier, may be ascribed to xenon either co-adsorbed with benzene within NaY(2.49) supercage with $4.7 < \theta < 5.0$ or adsorbed in the zeolite intercrystalline voids which may be surrounded by many benzene molecules. The top and bottom spectra in Fig. 6a represent respectively the raising and lowering of the sample 15 mm relative to the NMR coil. That only a single peak ($\delta = 74$ ppm) appears in the top spectrum (i.e. the bottom portion of the sample bed) and the disappearance of the same peak but with an additional sharp peak of gaseous xenon at $\delta \approx 0$ ppm in the bottom spectrum (i.e. the top portion of the sample bed), when compare with the middle spectrum, indicate the existence of a gradient of benzene concentration described above in case I. The same conclusion

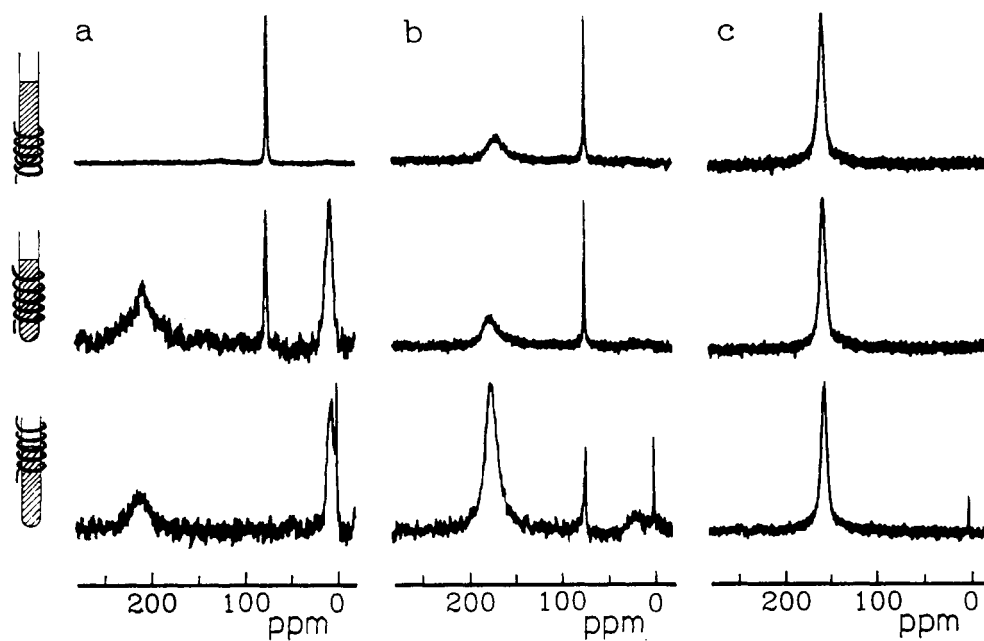


FIG. 6
Variation of ^{129}Xe NMR spectra (300 Torr xenon) of DBC benzene/NaY (2.49) sample with $\theta = 3.8$ recorded at various sample positions relative to the NMR coil (shown schematically on left) and under various preparatory conditions: a without treatment, b after mechanical mixing, and c after thorough thermal treatment (250°C , 10 h)

applies to the ^1H and ^{13}C NMR results obtained from the same sample, for which the ^{13}C NMR results are shown in Fig. 7a; the ^1H results resemble the ^{13}C results and hence are not shown. Spectra in Fig. 6b were the results taken after the same sample was shaken rigorously to perturb the concentration gradient. Except for the expected gas peak in the bottom spectrum, two major peaks at $\delta = 180$ and 74 ppm appear in all three sample positions which may be described as inhomogeneity of either case II or case III. The above statement is confirmed by the identical spectra shown in Fig. 6c which were recorded after treatment of the sample at 250°C for 10 h. After this thermal treatment, the low field ^{129}Xe peak at 180 ppm shifts up-field to ca 155 ppm which clearly indicate an homogeneous adsorbate distribution in the sample as shown in Fig. 5e. By comparison, ^1H and ^{13}C NMR data, although providing consistent information, are less sensitive to resolve the detailed states of adsorption of benzene; both ^{13}C (Fig. 7b) and ^1H NMR spectra obtained after sample shaking are almost invariant to the sample positions, and subsequent thermal treatment of the sample also resulted in change of neither NMR chemical shift nor linewidth. Based on the ^{129}Xe spectra in Fig. 6b alone, we cannot readily distinguish between cases II and III without a more detailed and quantitative study. Nevertheless, even though the sample had not yet reached a state of equilibrium, it is clear that sample shaking did promote adsorbate distribution within the zeolite

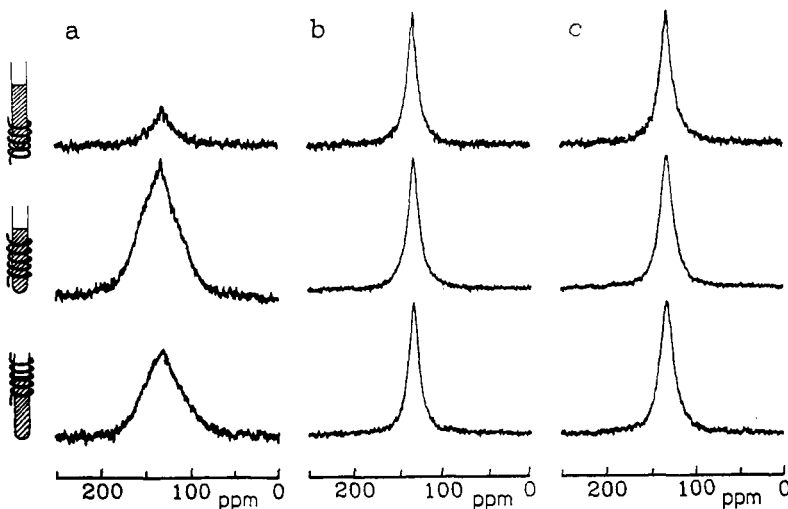


FIG. 7

Variation of ^{13}C NMR spectra of benzene adsorbed on NaY(2.49) zeolite with $\theta = 3.8$ recorded under various experimental and preparatory conditions: a DBC, without treatment, b DBC, after mechanical mixing, and c SBC, without treatment. The ^1H NMR spectra of benzene behave similarly

sample as indicated by the change of ^{129}Xe spectra in Fig. 6b and 6c; ^1H and ^{13}C results exemplified in Fig. 7b therefore only reflect an overall adsorbate distribution throughout the sample bed (i.e. case II, III or IV). The peak at $\delta \approx 180$ ppm in Fig. 6b which corresponds to $\theta \approx 4.2 - 4.5$ in the 'homogeneous' sample⁹ again indicates the preference of benzene molecules to adsorb collectively in either internal or external voids of NaY(2.49) before a truly homogeneous distribution is attained.

The effects of sample bed configuration on the adsorption and transport of benzene in faujasite-type zeolites have also been investigated. The variation of ^{129}Xe and ^{13}C NMR spectra on the SBC benzene/NaY(2.49) for $\theta = 3.8$ sample without treatment are shown in Fig. 8a and Fig. 7c, respectively. Before the NMR measurements, each sample prepared by SBC was transferred to the standard NMR sample tube after adsorption of benzene; a sample so prepared disturbed the initial adsorption states of the adsorbate. Hence, as far as the bulk benzene distribution in the sample bed is concerned, the SBC samples are equivalent to the DBC samples after mechanical mixing. Therefore, it is not surprising that the ^{13}C spectra in Fig. 7c resemble those in Fig. 7b, and similarly for the observed ^1H spectra. However, a notable difference has been observed between the ^{129}Xe spectra in Figs 8a and 6b; the spectra shown in Fig. 8a were obtained one week after adsorption of benzene. The major differences between spectra in Figs 8a and 6b are the disappearance of the 74 ppm peak (from xenon in the supercage in the absence of benzene) and the relative S/N ratios of the peak ca 170 ± 3 ppm at each detection position which

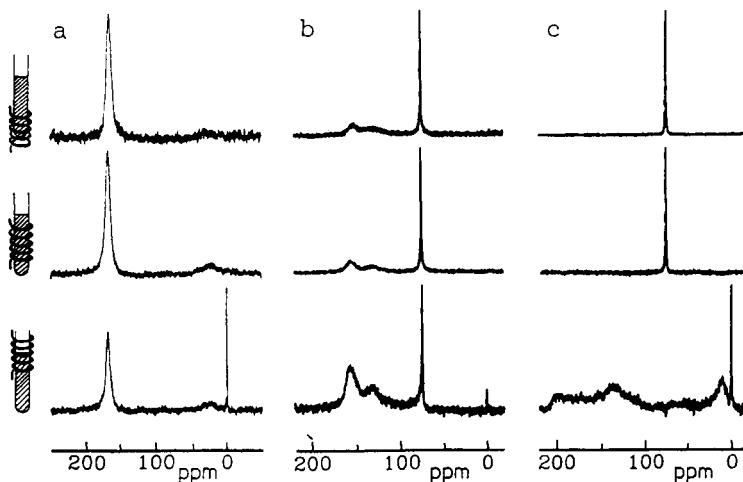


FIG. 8

Comparison of ^{129}Xe NMR spectra (300 Torr xenon) of different samples at different experimental positions without sample treatment, a SBC benzene/NaY(2.49) with $\theta = 3.8$, b SBC benzene/NaY(2.49); $\theta = 2.8$, and c DBC benzene/NaY(2.49); $\theta = 2.8$

indicate that the condition of equilibrium adsorption of benzene on NaY(2.49) zeolites depends strongly on the overall height of the sample bed. This argument is supported by the comparison of results in Figs 8b and 8c which are the corresponding ^{129}Xe spectra of SBC and DBC benzene/NaY(2.49) samples with $\theta = 2.8$ without thermal treatment. The fact that the ^{129}Xe resonance at 74 ppm is invisible in the bottom spectra of both Figs 6a and 8c indicated that in the DBC upon adsorption of benzene, benzene molecules are adsorbed on the uppermost layer of the sample bed. Furthermore, by comparing the relative intensities of the 74 ppm peak and the broad peak at low field in the normal detection position (middle spectrum of Figs 6a and 8c), we conclude that the adsorption front of benzene tends to migrate downward along the sample bed with increasing benzene coverage. In contrast, by comparing the bottom spectra in Figs 6a and 8c, we see that the chemical shift of the low field peak located typically at 160–220 ppm depends on the dosage of the adsorbate. Finally, by examining the difference between spectra in Figs 8a and 8b, we recognize the relative ease of obtaining a uniform adsorbate distribution at higher adsorbate loadings than lower adsorbate loadings.

The above discussed sorption and transport behaviors of benzene on NaY(2.49) zeolites also occurred when benzene molecules were adsorbed on zeolite adsorbate having varied Si/Al ratios. For instance, the ^1H and ^{129}Xe NMR spectra of a DBC

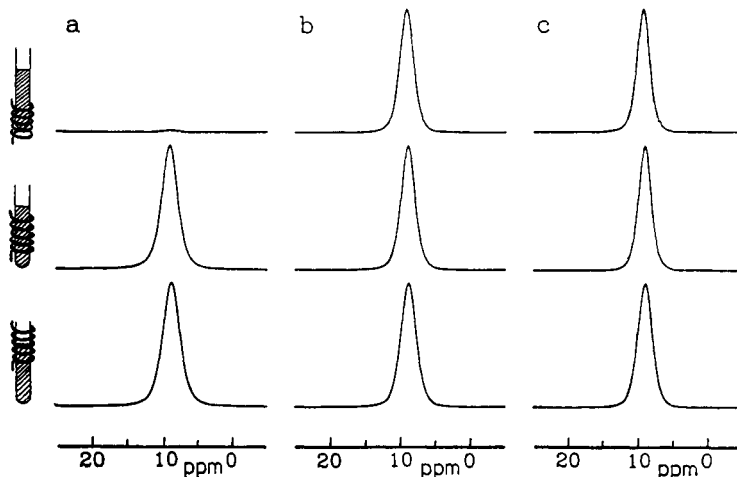


FIG. 9

Variation of ^1H NMR spectra of benzene adsorbed on DBC NaX(1.23) zeolite with $\theta = 2.0$ recorded under different experimental and preparatory conditions: a without treatment, b after mechanical mixing, and c after thorough thermal treatment (250°C , 10 h). The ^{13}C NMR spectra of benzene behave similarly

benzene/NaX(1.23) sample ($\theta = 2.0$), subjected to the same sample preparatory procedures and experimental conditions as for Figs 6a–6c, are displayed in Figs 9 and 10, respectively; ^{13}C NMR spectra which give similar information are not shown.

In summary, we have studied the adsorption properties of benzene on dehydrated NaX and NaY zeolites by ^{129}Xe , ^1H , and ^{13}C NMR spectroscopy. We found that a homogeneous benzene adsorption within the zeolite supercages depends not only on the benzene loading but also on the sample bed configuration. Upon adsorption of benzene onto the dehydrated zeolite samples at room temperature, benzene molecules tend to adsorb either within the supercages of the zeolite crystallites with a group of ca four molecules per supercage or on the external surface of the zeolite crystallite which may form zeolite aggregates on the accessible uppermost layer of the zeolite sample; in both cases a gradient of bulk concentration along the sample bed results. This effect, which depends only slightly on the Si/Al ratio of the zeolite adsorbents but strongly on the sample bed configuration, was also found to depend on the average benzene loading. Only after a protracted period does the overall benzene concentration become "uniform" throughout the sample bed at the macroscopic level. Although mechanical sample mixing accelerates the redistribution of benzene along the overall sample bed, it cannot ensure a homogeneous distribution within supercages of the faujasite-type zeolites. Thermal treatment of the benzene/zeolite sample at a temperature above 250°C for several hours is indis-

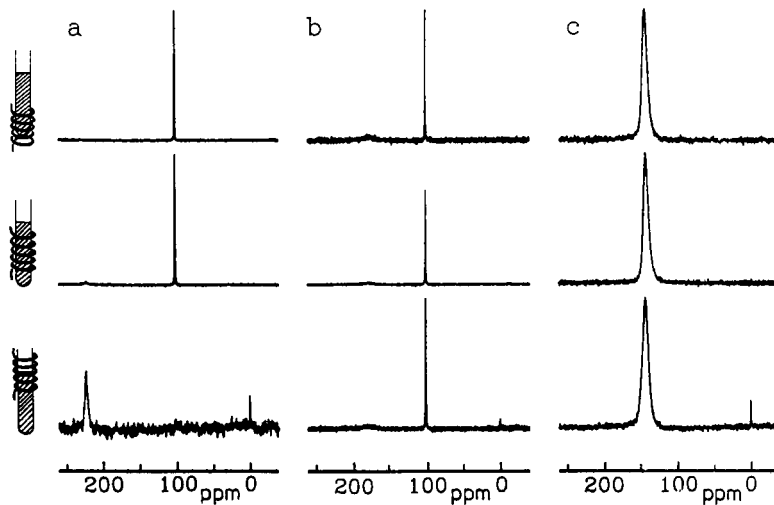


FIG. 10

Variation of ^{129}Xe NMR spectra (300 Torr xenon) obtained with the same DBC benzene/NaX(1.23) sample with $\theta = 2.0$ and under identical experimental and preparatory conditions as in Fig. 9

pensable to ensure a homogeneous sample distribution. The results obtained in this work show that one must be cautious in believing that, at room temperature, the equilibrium adsorption of benzene occurs naturally and rapidly in dehydrated faujasite-type zeolites. Moreover, with regard to the detailed adsorbate distribution, ^{129}Xe NMR of the coadsorbed xenon is much more sensitive than conventional ^1H or ^{13}C NMR of the adsorbed benzene.

The authors express their appreciation to Professor Hellmut G. Karge for helpful discussions and for his active interest in this work. The support of this work by the National Science Council of the Republic of China, grant No. NSC80-0208-M001-48, is gratefully acknowledged.

REFERENCES

1. de Menorval L. C., Raftery D., Liu S. B., Takegoshi K., Ryoo R., Pines A.: *J. Phys. Chem.* **94**, 27 (1990).
2. Chmelka B. F., Pearson J. G., Liu S. B., Ryoo R., de Menorval L. C., Pines A.: *J. Phys. Chem.* **95**, 303 (1991).
3. Wu J. F., Chen T. L., Ma L. J., Lin M. W., Liu S. B.: *Zeolites* **12**, 86 (1992).
4. Gedeon A., Ito T., Fraissard J.: *Zeolites* **8**, 376 (1988).
5. Karge H. G. (Fritz Haber Institute, Max Planck Society): Personal communication (1991).
6. Jameson C. J.: *J. Chem. Phys.* **6**, 5296 (1975).
7. Breck D. W.: *Zeolite Molecular Sieves: Structure, Chemistry, and Use*, p. 636. Wiley, New York 1974.
8. Raftery D., Long H., Meersmann T., Grandinetti P. J., Reven L., Pines A.: *Phys. Rev. Lett.* **66**, 584 (1991).
9. Liu S. B., Wu J. F., Ma L. J., Lin M. W., Chen T. L. in: *Proceedings of the 7th ROK/ROC Joint Symposium on Catalysis*, p. 184, KIST/KICHE, Seoul, Korea 1990; *J. Phys. Chem.*, submitted.
10. Primet M., Garbowski E., Mathieu M. V., Imelik B.: *J. Chem. Soc., Faraday Trans. 1* **76**, 1942 (1980).
11. Ito T., Fraissard J.: *J. Chem. Phys.* **76**, 5225 (1982).
12. Cheung T. T. P., Fu C. M., Wharry S.: *J. Phys. Chem.* **92**, 5170 (1988).
13. Ripmeester J. A., Davison D. W.: *J. Mol. Struct.* **75**, 67 (1981).
14. Ripmeester J. A.: *J. Am. Chem. Soc.* **104**, 289 (1982).
15. Stengle T. R., Reo N. V., Williamson K. L.: *J. Phys. Chem.* **85**, 3772 (1981).
16. Miller K. W., Reo N. V., Shoot Uiterkamp A. J. M., Stengle D. P., Stengle T. R., Williamson K. L.: *Proc. Natl. Acad. Sci. U.S.A.* **78**, 4946 (1981).
17. Barrer R. M., Bultitude F. W., Sutherland J. W.: *Trans. Faraday Soc.* **53**, 1111 (1957).
18. Lechert H., Wittern K.-P.: *Ber. Bunsenges. Phys. Chem.* **82**, 1054 (1978).
19. Kärger J., Caro J.: *J. Chem. Soc., Faraday Trans. 1* **9**, 1363 (1977).
20. Lee L.-K., Ruthven D. M.: *J. Chem. Soc., Faraday Trans. 1* **75**, 2406 (1979).
21. Yucel H., Ruthven D. M.: *J. Chem. Soc., Faraday Trans. 1* **76**, 71 (1980).
22. Kärger J., Kočík M., Zikánová A.: *J. Colloid Interface Sci.* **84**, 240 (1981).
23. Kärger J., Bülow M., Struve P., Kočík M., Zikánová A.: *J. Chem. Soc., Faraday Trans. 1*, **74**, 1210 (1978).
24. Bülow M., Struve P., Finger G., Redszus C., Ehrharst K., Schirmer W., Kärger J.: *J. Chem. Soc., Faraday Trans. 1* **76**, 597 (1980).
25. Kärger J., Heink W., Pfeifer H., Rauscher M., Hoffmann J.: *Zeolites* **2**, 275 (1982).